79-4040

Dynamic Response Analysis of Structural Systems Using a Direct Integration Method

J.S. Przemieniecki*
Air Force Institute of Technology, Wright-Patterson Air Force Base, Ohio
and
R.J. Talbot†
Aeronautical Systems Division, Wright-Patterson Air Force Base, Ohio

The main categories of numerical analyses of dynamical response of structural systems represented by finite elements are discussed and a direct integration method is derived using Padé approximations to the exact exponential series solutions. The method can be employed for the analysis of aircraft structures subjected to arbitrary time-dependent loading. Numerical stability, artificial attenuation, and phase shift of the approximate solutions are discussed in detail. The dynamic response solution is presented in the form of an explicit operator requiring only one inversion of the mass matrix of the system. A numerical example is included for the dynamic response of an elastic circular bar subjected to axisymmetric compressive stress at the free end. The numerical results are compared with a solution obtained by the finite difference method.

Nomenclature

$\boldsymbol{A}$ = matrix defined by Eq. (9)
$\boldsymbol{B}$ = $\boldsymbol{M}^{-1}\boldsymbol{K}$
$\boldsymbol{C}$ = damping matrix
$\boldsymbol{D}, \boldsymbol{D}_0 \boldsymbol{D}_1$ = approximation operators
$\boldsymbol{D}_{ij}$ = submatrices of the matrix $\boldsymbol{D}_p(h)$
D_{ij} = scalar coefficient derived from $\boldsymbol{D}_{ij}$
$\tilde{\boldsymbol{D}}$ = exact operator for the ith mode
$\boldsymbol{D}_p(h)$ = approximation operator
$\boldsymbol{D}_g(h)$ = approximation operator, defined by Eq. (24)
$\boldsymbol{F}$ = force matrix
$\boldsymbol{G}$ = forcing function matrix
$\boldsymbol{G}_p(h)$ = forcing function matrix
$\boldsymbol{I}$ = identity matrix
$\boldsymbol{K}$ = stiffness matrix
$\boldsymbol{M}$ = mass matrix
$\boldsymbol{P}$ = external load matrix
$\boldsymbol{Q}$ = matrix defined by Eq. (10)
R = attenuation factor
S = phase shift factor
T = exact period
$\tilde{T}$ = approximate period
T_m = period for the highest frequency
a, b = real and imaginary parts of λ
$g(\boldsymbol{B})$ = polynomial function of the matrix $\boldsymbol{B}$
h = $t - t_0$, time step
n = subscript for time t_0
$n+1$ = subscript for time $t_0 + h$
p, q = integers
$\boldsymbol{p}_i$ = elastic ith mode matrix
r = radial coordinate
$\boldsymbol{r}$ = $\{\boldsymbol{u}\dot{\boldsymbol{u}}\}$
$\tilde{\boldsymbol{r}}$ = $\{\tilde{\boldsymbol{u}}\dot{\tilde{\boldsymbol{u}}}\}$
$\boldsymbol{r}_c$ = complementary solution of Eq. (7)
$\boldsymbol{r}_p$ = particular solution of Eq. (7)
$\boldsymbol{r}_0$ = $\{\boldsymbol{u}_0 \dot{\boldsymbol{u}}_0\}$, initial values of $\boldsymbol{r}$ at $t = 0$
t = time
u = radial displacement
$\boldsymbol{u}$ = displacements
$\dot{\boldsymbol{u}}$ = velocities
$\ddot{\boldsymbol{u}}$ = accelerations
$\tilde{\boldsymbol{u}}$ = displacements in the ith mode
$\dot{\tilde{\boldsymbol{u}}}$ = velocities in the ith mode
w = longitudinal displacement
z = longitudinal coordinate
ϵ = error matrix
λ = coefficient (eigenvalue)
$\tilde{\lambda}$ = eigenvalue of the matrix $\tilde{\boldsymbol{D}}$
μ = coefficient
σ_z = longitudinal stress (compressive)
Φ_i = function of time for the ith mode
$\bar{\omega}$ = characteristic frequency
ω_i = ith characteristic frequency
$\tilde{\omega}$ = characteristic frequency in the approximation operator $\boldsymbol{D}_p(h)$

Introduction

THE basic equations of motion for a linear structural system represented by finite elements can be expressed by

$$\boldsymbol{M}\ddot{\boldsymbol{u}} + \boldsymbol{C}\dot{\boldsymbol{u}} + \boldsymbol{K}\boldsymbol{u} = \boldsymbol{P} \tag{1}$$

where $\boldsymbol{M}$ is the mass matrix, $\boldsymbol{C}$ is the damping matrix, $\boldsymbol{K}$ is the stiffness matrix, and $\boldsymbol{u}$, $\dot{\boldsymbol{u}}$, and $\ddot{\boldsymbol{u}}$ represent the nodal displacement, velocity, and acceleration vectors, respectively. For nonlinear systems, $\boldsymbol{M}$, $\boldsymbol{C}$, and $\boldsymbol{K}$ may be dependent on the displacements $\boldsymbol{u}$. The matrix $\boldsymbol{P}$ represents time-dependent external forces applied to the structural system. The different methods used to obtain the transient response of a system represented by Eq. (1) may be divided into three main categories: modal analysis, finite time elements, and direct time integration. The present paper reviews briefly these main categories and discusses an analysis method based on the matrix series approximation to the exact solution. The method presented can be used for the analysis of aircraft structures subjected to arbitrary time-dependent loading.

In modal analysis, response of a structural system is expressed as a linear combination of rigid body modes and elastic modes of vibration with some appropriate time-dependent multipliers for the individual modes (see, for example, Ref. 1). The use of a large number of modes is not particularly efficient from the computational point of view

Received April 3, 1978; revision received Aug. 16, 1978. Copyright © American Institute of Aeronautics and Astronautics, Inc., 1978. All rights reserved.

Index category: Structural Dynamics.

*Dean, School of Engineering. Associate Fellow AIAA.
†Air Force On-site Representative, Lockheed-California Co., Burbank, Calif.

and therefore the technique is generally used only when a limited number of low-frequency modes would be adequate for the solution. Since an arbitrary exciting force P can affect all modes of the system, the modal analysis method must always be used judiciously to avoid serious inaccuracies when higher modes are also involved in the response.

The fundamental concepts of the finite time element method were discussed by Fried,[2] Argyris and Scharpf,[3] and Oden.[4] This technique extends the spatial discretization method of matrix structural analysis to the time domain; however, the technique has the distinct disadvantage of greatly increasing the number of generalized coordinates required to describe the system. For example, if third-order Hermitian interpolation polynomials are used in the time interpolation process, the number of generalized coordinates will be four times greater than the number of spatial degrees of freedom. The solution of equations of motion therefore requires inversion of extremely large space-time matrices.

The direct integration method includes the whole range of techniques such as finite difference solutions, computational algorithms based on approximation of motion within a time interval, or approximations to the exact series solution. The use of any of these techniques requries consideration of their stability characteristics. Three possibilities exist: the technique is unstable, i.e., it produces a solution with unbounded error for any length of time step; it is conditionally stable, i.e., the solution is bounded for some range of values of the time step and unbounded otherwise; or it is unconditionally stable. The last condition is highly desirable but not necessarily of paramount importance because these techniques have yet another characteristic, that of introducing artificial attenuation and/or phase shift in the solution. Even in the case of unconditionally stable methods, the time step should be limited in order to minimize the effect of phase shift.

In the direct methods many different algorithms have been used in the past based on either single or multistep formulation. Some of the more common ones are the generalized acceleration methods which involve algorithms derived from the assumption of constant, linear, or two-step variation of acceleration over the specified time interval. Nickell reviewed several of the direct integration techniques and pointed out that considerable judgment is required in their use and in the interpretation of the occasionally unexpected results.[5] To alleviate this problem, considerable effort has been expended in the past in examining the stability characteristics of these techniques. Thus the work of Nickell cited above investigated the stability of the Newmark generalized acceleration method, the Wilson averaging operator, and the Gurtin variational method. Leech et al.[6] demonstrated the conditional stability of the standard central difference technique while Johnson[7] demonstrated the unconditional stability of the Houbolt method. Nevertheless, the selection and application of one of the direct integration methods remain difficult problems. Nickell summarized the situation very well when he stated that[5]:

> Practitioners of the art who are able to judiciously select time step size in order to achieve the elusive objectives of solution stability and reasonable computation time are scarce. Occasional spurious results often defy careful post-computation analysis.
>
> It would seem clear, then, that if finite element techniques are to achieve the same goals in dynamic stress analysis that have been achieved in static stress analysis, an improved rationale for treating the temporal variation should be sought.

More recently Geradin[8] studied the various approximation methods available to carry out the integration of the equations of motion of structural systems. In his study a comparison of the various schemes was made on the basis of their accuracy, stability, and computer implementation.

Since the basic equations of motion for a linear system can be solved in terms of an exponential matrix series, another class of algorithms can be derived from Padé approximation of exp (Ah) where the matrix A is expressed in terms of the matrices M, C, and K and h is the time step. The direct integration of linear equations of motion using some of the Padé approximations was discussed by Trujillo.[9] The integration scheme discussed in the present paper is based on the truncated exact matrix series which, in fact, is a special case of Padé approximations.

Another method deserving special recognition was developed by Argyris et al.[10] The method is unconditionally stable and its algorithm is obtained by interpolating the inertia forces $M\ddot{u}$ as Hermitian polynomials. This leads to the matrix equation

$$D_1 r_{n+1} = D_0 r_n + F \tag{2}$$

from which

$$r_{n+1} = D_1^{-1} D_0 r_n + D_1^{-1} F \tag{3}$$

Different order Hermitian polynomials may be used in this approximation. In Eq. (2) both D_1 and D_0 are matrices of the order $2n \times 2n$, where n is the number of the degrees of freedom. Each matrix element in D_1 or D_0 is represented by a power series in h with the number of terms depending on the order of the Hermitian polynomials used for the interpolation. The remaining matrices in Eq. (2) are defined by

$$r_{n+1} = \{u_{n+1} \dot{u}_{n+1}\} \tag{4}$$

and

$$r_n = \{u_n \dot{u}_n\} \tag{5}$$

while the force matrix F is obtained in terms of known forces and their time derivatives at times n and $n+1$. As mentioned before, this method has the inherent advantage of unconditional stability but its disadvantage lies in the large order matrices $(2n \times 2n)$ required for inversion in Eq. (3). It should also be noted that this method is analogous to Padé approximations for even combinations (see Ref. 7). By contrast to Eq. (3), the method described in the present paper leads to the solution in an explicit form

$$r_{n+1} = D r_n + GP \tag{6}$$

which does not require any large size matrix inversion; however, the method is only conditionally stable limiting the maximum size of the time step h.

Series Solution

Equation (1) can be combined with the identity $\dot{u} = \dot{u}$ to form a first-order differential equation

where

$$\dot{r} = Ar + Q \tag{7}$$

$$r = \{u \ \dot{u}\} \tag{8}$$

$$A = \begin{bmatrix} 0 & I \\ -M^{-1}K & -M^{-1}C \end{bmatrix} \tag{9}$$

$$Q = \begin{bmatrix} 0 \\ M^{-1}P \end{bmatrix} \tag{10}$$

Thus the system of n-coupled second-order differential equations is replaced by a system of $2n$ first-order differential equations. The mass matrix M is usually nonsingular. For some structural problems for which concentrated masses are associated only with certain degrees of freedom the matrix M will be singular. In these cases, a condensed stiffness matrix can be used to render M nonsingular.[11]

The complementary solution of Eq. (7) is given by[12]

$$r_c = e^{At} r_0 \tag{11}$$

where r_0 is a column matrix of the initial values of r when $t=0$. The expression e^{At} is given by the matrix series

$$e^{At} = I + At + \tfrac{1}{2}!A^2t^2 + \ldots + \frac{1}{q!}A^q t^q \tag{12}$$

which is absolutely and uniformly convergent.

The particular solution is obtained by multiplying both sides of Eq. (7) by $\exp(-At)$ which leads to

$$\frac{\mathrm{d}}{\mathrm{d}t}(e^{-At} r) = e^{-At} Q(t) \tag{13}$$

Hence

$$r_p = e^{At} \int_{s=0}^{s=t} e^{-As} Q(s)\,\mathrm{d}s \tag{14}$$

Addition of the modified Eq. (11), where the time t is measured from t_0, and Eq. (14) leads to the complete solution in the form

$$r = e^{A(t-t_0)} r_0 + e^{At} \int_{s=t_0}^{s=t} e^{-As} Q(s)\,\mathrm{d}s \tag{15}$$

where

$$r_0 = \{u_0 \dot{u}_0\} \tag{16}$$

denotes the column of displacements u and velocities $\dot{u}$ at $t=t_0$. It should be noted that the time variable is continuous in Eq. (15) and that no approximations have been made so far to the solution.

If the time interval $t-t_0$ is small, $Q(s)$ may be assumed as constant over this interval which allows for the integration of Eq. (15) so that

$$r = e^{A(t-t_0)} r_0 - (I - e^{A(t-t_0)}) A^{-1} Q_n \tag{17}$$

where Q_n is the average value of $Q(s)$ over the time interval $t-t_0$. For greater accuracy a linear variation of $Q(s)$ over the interval can be assumed.

Finite Step Solution

The finite step solution is obtained directly from Eq. (17) by designating subscripts n and $n+1$ to denote times t_0 and t. Hence

$$r_{n+1} = e^{Ah} r_n - (I - e^{Ah}) A^{-1} Q_n \tag{18}$$

where

$$h = t - t_0 \tag{19}$$

For numerical computations a truncated matrix series expression can be used in Eq. (18) so that

$$r_{n+1} = D_p(h) r_n - (I - D_p(h)) A^{-1} Q_n \tag{20}$$

where

$$D_p(h) = I + Ah + \tfrac{1}{2}!A^2h^2 + \ldots + \frac{1}{p!}A^P h^P \tag{21}$$

The inverse of A^{-1} can be obtained from Eq. (9) as

$$A^{-1} = \begin{bmatrix} -K^{-1}C & -K^{-1}M \\ I & 0 \end{bmatrix} \tag{22}$$

which clearly does not exist unless the stiffness matrix is nonsingular. Thus Eq. (20) as written cannot be used to solve for structural responses including the rigid body motion. For these cases the integration in Eq. (15) must be performed by substituting the series expansion for $\exp(-As)$ and integrating term by term. This leads to

$$r_{n+1} = D_p(h) r_n + D_q(h) Q_n \tag{23}$$

where

$$D_q(h) = h\left(I + \tfrac{1}{2}!Ah + \tfrac{1}{3}!A^2h^2 + \ldots + \frac{1}{(q+1)!}A^q h^q\right) \tag{24}$$

and

$$q = p - 1 \tag{25}$$

For systems for which K is nonsingular, a further simplification of Eq. (20) is possible. When Eqs. (10) and (22) are substituted into Eq. (20), it follows that

$$r_{n+1} = D_p(h) r_n + G_p(h) P \tag{26}$$

where

$$G_p(h) = \begin{bmatrix} (I - [D_{11}]_{n\times n}) \\ -[D_{21}]_{n\times n} \end{bmatrix} K^{-1} \tag{27}$$

where the matrices $[D_{ij}]$ are the indicated partitions of $D_p(h)$.

Padé Approximations

The exact series solution $\exp(Ah)$ can also be approximated using modified Pade approximation in the form[13]

$$e^{Ah} \approx \left(\sum_{k=0}^{q} \frac{(p+q-k)!q!}{(p+q)!k!(q-k)!}(-A)^k h^k\right)^{-1} \times \sum_{k=0}^{p} \frac{(p+q-k)!p!}{(p+q)!k!(p-k)!} A^k h^k \tag{28}$$

When values of p and $q=0$, 1, 2 are substituted into Eq. (28), a table of Padé approximations can be generated as shown in Table 1. Clearly the case $p=q=0$ cannot be used as an approximation since it does not allow for any changes over the time step h.

The case $p=1$, $q=0$ is, in fact, the forward difference explicit formula, while $p=0$, $q=1$ represents the backward difference implicit formula. Another approximation from the Padé table used extensively in numerical computations is for $p=q=1$ which is referred to as the Crank-Nicholson formula. The algorithm derived by Argyris et al.[10] is of the form similar to the case $p=q$ in which both the inverted matrix and the multiplicant matrix consist of a sum of matrix terms with like powers of h. In this paper, solutions of Eqs. (20) or (26) will be based on Padé approximations for $q=0$. However, only solutions with $p \geq 3$ can provide a conditionally stable algorithm for the numerical solution.

Stability, Attenuation, and Phase Shift

Stability (Error Propagation)

The stability analysis follows the procedure developed by O'Brien et al.[14] The analysis is based on the assumption that propagation of error ϵ from time t to $t+h$ (from n to $n+1$) is given by

$$\epsilon_{n+1} = e^{\mu h} \epsilon_n = \lambda \epsilon_n \tag{29}$$

Table 1 Padé approximations of exp (*Ah*)

	$p=0$	$p=1$	$p=2$
$q=0$	I	$I+Ah$	$I+Ah+\frac{1}{2}A^2h^2$
$q=1$	$(I-Ah)^{-1}$	$\left(I-\frac{1}{2}Ah\right)^{-1}\left(I+\frac{1}{2}Ah\right)$	$\left(I-\frac{1}{3}Ah\right)^{-1}\times\left(I+\frac{2}{3}Ah+\frac{1}{6}A^2h^2\right)$
$q=2$	$\left(I-Ah+\frac{1}{2}A^2h^2\right)^{-1}$	$\left(I-\frac{2}{3}Ah+\frac{1}{6}A^2h^2\right)^{-1}\times\left(I+\frac{1}{3}Ah\right)$	$\left(I-\frac{1}{2}Ah+\frac{1}{12}A^2h^2\right)^{-1}\times\left(I+\frac{1}{2}Ah+\frac{1}{12}A^2h^2\right)$

where ϵ_n is an arbitrary vector while μ and λ are coefficients to be determined. When ϵ_n is substituted for r_n in Eq. (20) with $Q_n=0$ it follows from Eq. (29) that

$$\epsilon_{n+1}=D_p(h)\epsilon_n=\lambda\epsilon_n \tag{30}$$

Hence

$$(D_p(h)-\lambda I)\epsilon_n=0 \tag{31}$$

For $\epsilon_n\neq 0$, Eq. (31) is satisfied when the stability determinant

$$|D_p(h)-\lambda I|=0 \tag{32}$$

where λ can now be interpreted as the eigenvalue of the approximation operator $D_p(h)$. An alternative form of Eq. (32) can be derived in terms of square submatrices in $D_p(h)$. The approximation operator $D_p(h)$ can be partitioned into four square submatrices so that Eq. (31) can be written as

$$\begin{bmatrix} (D_{11}-\lambda I) & D_{12} \\ D_{21} & (D_{22}-\lambda I) \end{bmatrix}\begin{bmatrix} \epsilon \\ \dot{\epsilon} \end{bmatrix}_n=\begin{bmatrix} 0 \\ 0 \end{bmatrix} \tag{33}$$

Hence

$$\dot{\epsilon}=-D_{12}^{-1}(D_{11}-\lambda I)\epsilon \tag{34}$$

and

$$(-\lambda^2 I+\lambda(D_{11}+D_{12}D_{22}D_{12}^{-1})-D_{12}D_{22}D_{12}^{-1}D_{11}+D_{12}D_{21})\epsilon=0 \tag{35}$$

which leads to the new stability determinant

$$|-\lambda^2 I+\lambda(D_{11}+D_{12}D_{22}D^{-1})-D_{12}D_{22}D_{12}^{-1}D_{11}+D_{12}D_{21}|=0 \tag{36}$$

For the subsequent analysis a new matrix

$$B=M^{-1}K \tag{37}$$

can be introduced. Examination of the operator $D_p(h)$ [see Eqs. (9) and (21)] for $C=0$ reveals that the component submatrices D_{ij} in $D_p(h)$ are represented by polynomials in B. This means that the stability determinant for an undamped system is of the form

$$|g(B)-\lambda^2 I|=0 \tag{38}$$

where

$$\begin{aligned} g(B)&=\lambda(D_{11}+D_{12}D_{22}D_{12}^{-1})-D_{12}D_{22}D_{12}^{-1}D_{11}+D_{12}D_{21} \\ &=\lambda(D_{11}+D_{22})-D_{22}D_{11}+D_{12}D_{21} \end{aligned} \tag{39}$$

is a polynomial function of the matrix B. The simplification represented by the second line of Eq. (39) is possible because the matrices D_{ij} are polynomials in B and therefore their matrix products are commutable.

From the theory of characteristic roots of a polynomial function of a matrix it follows that Eq. (38) can be rewritten as[15]

$$\begin{aligned} |g(B)-\lambda^2 I|&=(-1)^n(\lambda^2-g(\omega_1^2))(\lambda^2-g(\omega_2^2))\ldots \\ &(\lambda^2-g(\omega_i^2))\ldots(\lambda^2-g(\omega_n^2))=0 \end{aligned} \tag{40}$$

since the eigenvalues of the matrix B are equal to ω_i^2, where ω_i is the ith characteristic frequency of vibration of the undamped system.

The eigenvalues of the approximation operator $D_p(h)$ can now be calculated from Eq. (40) as functions of ω_i and h. Noting that $g(\omega^2)$ is now an algebraic expression

$$g(\omega^2)=\lambda(D_{11}+D_{22})-D_{11}D_{22}+D_{12}D_{21} \tag{41}$$

where D_{ij} are coefficients derived from D_{ij} when B is replaced with ω^2. Substitution of Eq. (41) into Eq. (40) leads to the following stability equation

$$\lambda^2-\lambda(D_{11}+D_{22})+D_{11}D_{22}-D_{12}D_{21}=0 \tag{42}$$

Hence

$$\lambda=\tfrac{1}{2}\{(D_{11}+D_{22})\pm i[-(D_{11}-D_{22})^2-4D_{12}D_{21}]^{\frac{1}{2}}\} \tag{43}$$

provided

$$-(D_{11}-D_{22})^2-4D_{12}D_{21}\geq 0 \tag{44}$$

When the above condition is satisfied the eigenvalues are complex conjugates.

From Eq. (29) it is clear that the requirement for stability is simply that the spectral radius of the approximation operator must be bounded by unity for the entire time interval h, i.e.,

$$\max|\lambda|\leq 1 \tag{45}$$

Hence it follows from Eqs. (43) and (45) that the following relationship must be satisfied.

$$(D_{11}D_{22}-D_{12}D_{21})^{\frac{1}{2}}\leq 1 \tag{46}$$

Attenuation and Phase Shift

The approximate nature of the operator $D_p(h)$ introduces an artificial attenuation and phase shift in the calculated dynamic response of an undamped structural system. This attenuation and phase shift can be studied by comparing the approximate solution with a known exact solution to a particular excitation of the system. It is well known that for a motion in a single characteristic mode (ith mode) the exact

displacements $\tilde{u}$ are given by

$$\tilde{u} = p_i \Phi_i(t) \tag{47}$$

where p_i is the ith elastic mode matrix (column vector) of the system and $\Phi_i(t)$ is a function of time. From Ref. 16

$$\tilde{u} = p_i \cos\omega_i t \Phi_i(0) + p_i \omega_i^{-1} \sin\omega_i t \dot{\Phi}_i(0) \tag{48}$$

where an overdot denotes the time derivative. Hence the velocities $\dot{\tilde{u}}$ are given by

$$\dot{\tilde{u}} = -p_i \omega_i \sin\omega_i t \Phi_i(0) + p_i \cos\omega_i t \dot{\Phi}_i(0) \tag{49}$$

Noting that

$$\tilde{u}(0) = p_i \Phi_i(0) \tag{50}$$

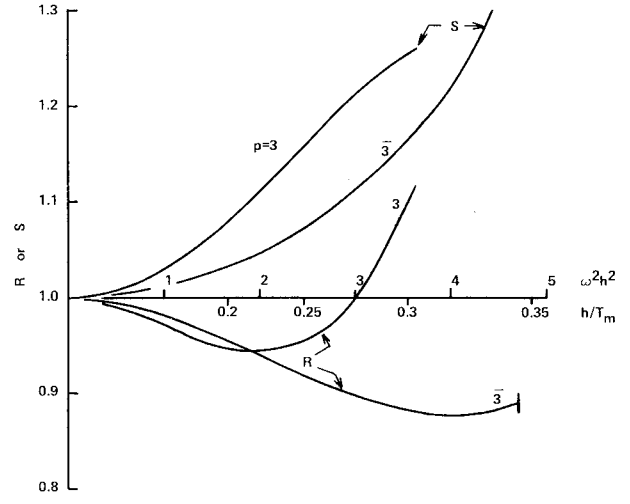

Fig. 1 Attenuation factor R and phase shift factor S for $p=3$ and $p=\bar{3}$ (modified).

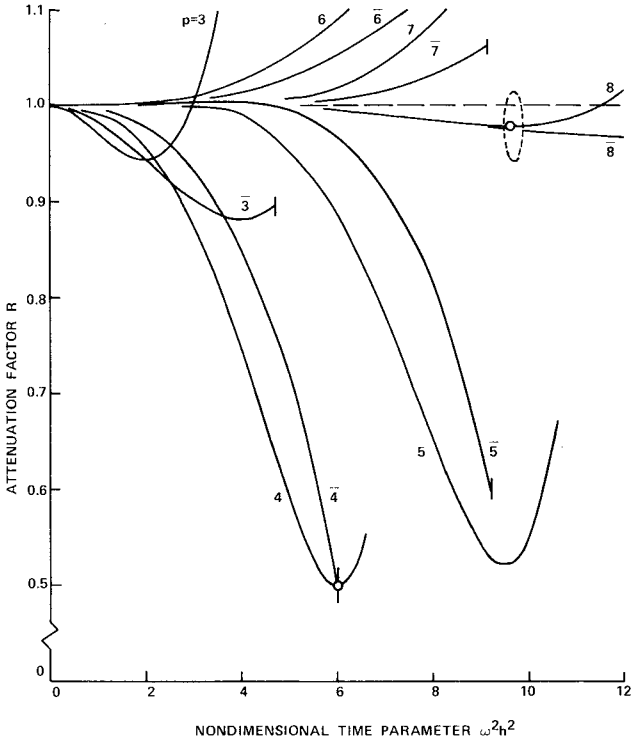

Fig. 2 Variation of attenuation factor R with $\omega^2 h^2$ (low values of p).

and

$$\dot{\tilde{u}}(0) = p_i \dot{\Phi}_i(0) \tag{51}$$

it follows that Eqs. (48) and (49) can be combined into one equation relating displacements and velocities at n and $n+1$. Hence

$$\begin{bmatrix} \tilde{u}_{n+1} \\ \dot{\tilde{u}}_{n+1} \end{bmatrix} = \begin{bmatrix} \cos\omega_i hI & \omega_i^{-1}\sin\omega_i hI \\ -\omega_i \sin\omega_i hI & \cos\omega_i hI \end{bmatrix} \begin{bmatrix} \tilde{u}_n \\ \dot{\tilde{u}}_n \end{bmatrix} \tag{52}$$

or

$$\tilde{r}_{n+1} = \tilde{D} r_n \tag{53}$$

where

$$\tilde{r}_{n+1} = \{\tilde{u}_{n+1}\, \dot{\tilde{u}}_{n+1}\} \tag{54}$$

$$\tilde{r}_n = \{\tilde{u}_n\, \dot{\tilde{u}}_n\} \tag{55}$$

and

$$\tilde{D} = \begin{bmatrix} \cos\omega_i hI & \omega_i^{-1}\sin\omega_i hI \\ -\omega_i \sin\omega_i hI & \cos\omega_i hI \end{bmatrix} \tag{56}$$

The eigenvalues $\tilde{\lambda}$ of the exact operator $\tilde{D}$ are determined from

$$|\tilde{D} - \tilde{\lambda} I| = 0 \tag{57}$$

Noting that the eigenvalues of I in $\tilde{D}$ are unity it follows immediately by the same reasoning which led to Eq. (42) that

$$\tilde{\lambda}^2 - 2\tilde{\lambda}\cos\omega_i h + 1 = 0 \tag{58}$$

Hence

$$\tilde{\lambda} = \cos\omega_i h \pm i \sin\omega_i h \tag{59}$$

The exact eigenvalues $\tilde{\lambda}$ can now be compared with the eigenvalues λ of the approximation operator $D_p(h)$. To accomplish this, Eq. (43) is rewritten as

$$\lambda = a \pm ib \tag{60}$$

$$= (a^2+b^2)^{1/2}\left(\frac{a}{(a^2+b^2)^{1/2}} \pm \frac{ib}{(a^2+b^2)^{1/2}}\right) \tag{60a}$$

$$= R(\cos\bar{\omega}h \pm i\sin\bar{\omega}h) \tag{60b}$$

where

$$a = \tfrac{1}{2}(D_{11} + D_{22}) \tag{61}$$

$$b = \tfrac{1}{2}[-(D_{11} - D_{22})^2 - 4D_{12}D_{21}]^{1/2} \tag{62}$$

$$R = (a^2+b^2)^{1/2} \tag{63}$$

The coefficient R is the attenuation factor which is also equal to the spectral radius of the approximation operator and $\bar{\omega}$ is the circular frequency of the approximation operator. From Eq. (60b) it follows that

$$\bar{\omega}h = \tan^{-1} b/a \tag{64}$$

Hence the ratio of the approximate to the exact frequency (phase shift factor) can be expressed by

$$S = \frac{\bar{\omega}}{\omega} = \frac{1}{\omega h}\tan^{-1} b/a \tag{65}$$

If necessary the period elongation in the approximate solution expressed as percentage of the exact value can be obtained from

$$\frac{\bar{T}-T}{T}\times 100\% = \left(\frac{2\pi}{\bar{\omega}}-\frac{2\pi}{\omega}\right)\times 100\% = \left(\frac{1}{S}-1\right)\times 100\% \quad (66)$$

The stability condition expressed by Eq. (45) imposes the requirement that $R \leqq 1$. Ideally the operator $D_p(h)$ should have eigenvalues for which both R and S are very closely equal to unity; however, this is not possible with the approximate solutions. In the next two sections the values of R and S will be discussed for the class of solutions based on Padé approximations

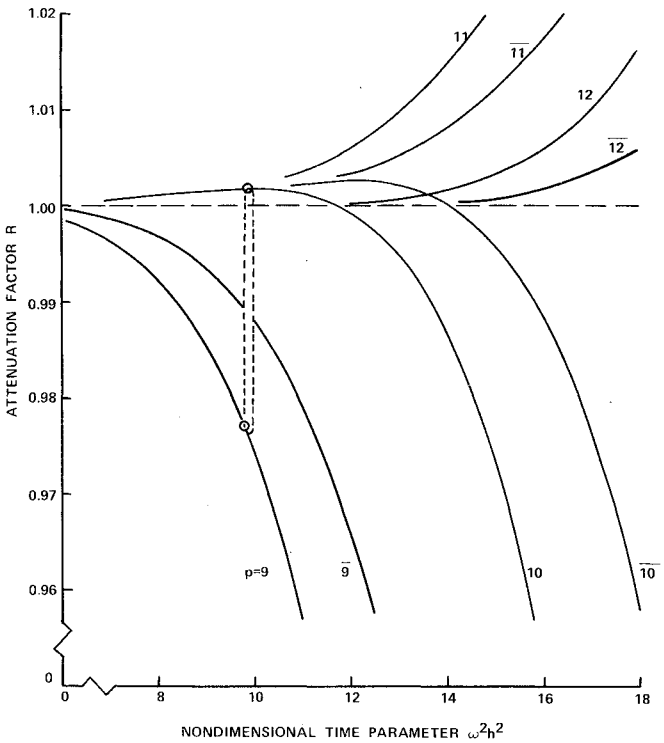

Fig. 3 Variation of attenuation factor R with ω^2h^2 (high values of p).

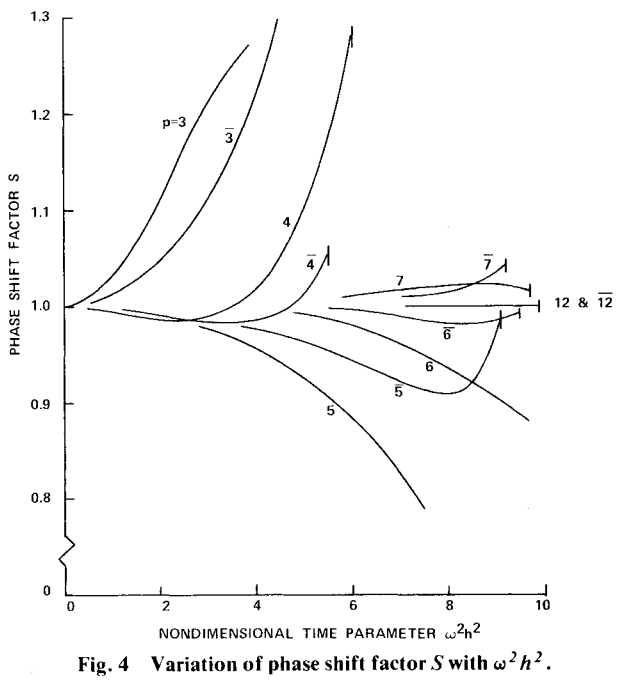

Fig. 4 Variation of phase shift factor S with ω^2h^2.

Attenuation and Phase Shift for $q=0$ and $p=1, 2, 3...12$

As mentioned in the Introduction, Padé approximations for $q=0$ are very attractive because the approximation operator $D_p(h)$ is given in an explicit form. To study the attenuation and phase shift in the solution, the matrix A appearing in the approximation operator must be determined for zero damping, i.e., $C=0$. This leads to the matrix A given by

$$A = \begin{bmatrix} 0 & I \\ -B & 0 \end{bmatrix} \quad (67)$$

It can be demonstrated that for $q=0$ and $p=1$ or 2 the attenuation factor R is greater than one, and therefore these approximations produce instability and cannot be used in any numerical calculations. For $q=0$ and $p \geqq 3$ the approximation operator $D_p(h)$ produces solutions which are conditionally stable. This restricts the maximum size of the time increment h for which $R<1$.

The determination of the attenuation factor R and the phase shift S will now be demonstrated for the specific case of $p=3$. From Eq. (21) it follows that for $p=3$

$$D_p(h) = I + Ah + \frac{1}{2}A^2h^2 + \frac{1}{6}A^3h^3 \quad (68)$$

Substituting Eq. (67) into Eq. (68) the above equation can be written as

$$D_p(h) = \begin{bmatrix} \left(I-\frac{1}{2}Bh^2\right) & \left(Ih-\frac{1}{6}Bh^3\right) \\ \left(-Bh+\frac{1}{6}B^2h^3\right) & \left(I-\frac{1}{2}Bh^2\right) \end{bmatrix} \quad (69)$$

Hence

$$D_{11} = D_{22} = I-\frac{1}{2}Bh^2 \quad (70)$$

$$D_{12} = Ih-\frac{1}{6}Bh^3 \quad (71)$$

$$D_{21} = -Bh+\frac{1}{6}B^2h^3 \quad (72)$$

$$D_{11} = D_{22} = 1-\frac{1}{2}\omega^2h^2 \quad (70a)$$

$$D_{12} = h\left(1-\frac{1}{6}\omega^2h^2\right) \quad (71a)$$

$$D_{21} = \frac{1}{h}\left(-\omega^2h^2+\frac{1}{6}\omega^4h^4\right) \quad (72a)$$

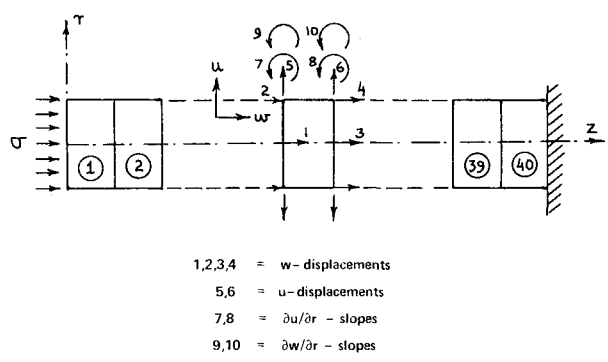

Fig. 5 Finite element model for transient response analysis of circular bar.

Substituting Eqs. (70a, 71a, and 72a) into Eq. (43)

$$\lambda = \left(1 - \frac{\omega^2 h^2}{2}\right) \pm i\left(\omega^2 h^2 - \frac{1}{3}\omega^4 h^4 + \frac{1}{36}\omega^6 h^6\right)^{1/2} \tag{73}$$

The attenuation factor R can now be calculated using the real and imaginary parts of λ as indicated by Eqs. (63) and (65). This leads to

$$R = \left(1 - \frac{1}{12}\omega^4 h^4 + \frac{1}{36}\omega^6 h^6\right)^{1/2} \tag{74}$$

and

$$S = \frac{1}{\omega h}\tan^{-1}\left\{\left(\omega^2 h^2 - \frac{1}{3}\omega^4 h^4 + \frac{1}{36}\omega^6 h^6\right)^{1/2} \Big/ \left(1 - \frac{\omega^2 h^2}{2}\right)\right\} \tag{75}$$

The variation of R with $\omega^2 h^2$ for $p = 3$ is plotted in Fig. 1. R is less than unity when $0 < \omega^2 h^2 < 3$. Ideally the value of R should not be less than 0.999 to produce a minimal amount of artificial attenuation. Thus for $p = 3$ the value of R within the admissible range of ωh makes this particular Padé approximation unacceptable. Similarly, the phase shift factor S increases rapidly with increasing ωh as shown in Fig. 1 which causes an additional error. The horizontal scale in Fig. 1 includes both $\omega^2 h^2$ and h/T_m, where T_m is the period of the highest frequency in the system.

A simple modification can be made to the solution by including some additional higher order terms in the expansions for the submatrices D_{11} and D_{12} of the operator $D_p(h)$ so that D_{21} and D_{22} become exact time derivatives of D_{11} and D_{12}, respectively. For example, the modified form of Eq. (69) would become

$$D_p(h) = \begin{bmatrix} \left(I - \frac{1}{2}Bh^2 + \frac{1}{24}B^2h^4\right) & \left(Ih - \frac{1}{6}Bh^3\right) \\ \left(-Bh + \frac{1}{6}B^2h^3\right) & \left(I - \frac{1}{2}Bh^2\right) \end{bmatrix} \tag{76}$$

The variations of R and S with $\omega^2 h^2$ for $p = 3$ (modified) are also plotted in Figs. 1 and 2. Although here the range of $\omega^2 h^2$ for which $R < 1$ has been extended by comparison with the $p = 3$, no significant improvement in accuracy is achieved by this modification. It should be noted that in this case for $\omega^2 h^2 > 4.72$ the eigenvalues λ become real.

A computer program has been used to determine variation of R and S with $\omega^2 h^2$ for values of $p = 3,4,5 \ldots 12$, including in each case the modified version of the approximation operator $D_p(h)$. The results are shown in Figs. 2, 3, and 4. For certain values of ωh the eigenvalues λ of the approximation operator converge to a repeated real root, e.g., $p = 4$ (modified) at $\omega^2 h^2 = 6$ which is represented by a small circle in Fig. 2. In some cases the eigenvalues become a pair of real numbers as indicated by vertical bars across the R curves in Figs. 2 and 3. For $p = \bar{8}$ and $p = \bar{9}$ (bars over numbers indicate here the modified operators), the absolute values of the pair of real eigenvalues are plotted to indicate that the real roots in these cases extend over a small range of ωh and that the numerical solutions for this range are unstable since the spectral radius is greater than one. In Fig. 4 the phase shift factor S is plotted for various values of p for the range of ωh for which the eigenvalues are complex conjugates.

Examination of Fig. 3 indicates clearly that if an attenuation error of 0.1% or less is desirable the approximation operator $D_p(h)$ for $p = 12$ or $p = \bar{12}$ (modified) should be used while the time step should be restricted to $\omega^2 h^2 < 9.8$. Similarly, from Fig. 4, to have no more than 1% error in the phase shift S approximation operators for at least $p = 9$ should be used.

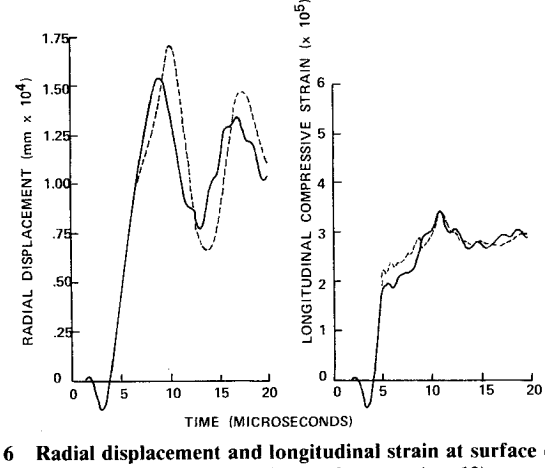

Fig. 6 Radial displacement and longitudinal strain at surface of bar at $z = 25.40$ mm (1 in.). ——, finite elements ($p = 12$); ----, finite difference (Ref. 17).

Numerical Example

The analysis method developed in this paper has been applied to the study of wave propagation in a finite length elastic circular bar. The bar was assumed to be fixed both longitudinally and radially at one end. The opposite end was unconstrained and the bar was initially at rest. At $t = 0$ an axisymmetric compressive stress $\sigma_z = 2.0684$ MPa (300 lb/in.^{2}) represented by a step function was applied to the free end. The physical properties of the bar are given in Table 2.

The analysis has been performed using the approximation operator $D_p(h)$ for $p = 12$. The finite element model used in the analysis is shown in Fig. 5. The length of the bar has been divided into 40 equal length elements. Special stiffness and mass matrices have been developed for the ten degree-of-freedom element illustrated in Fig. 5. The axisymmetric displacement field for the element has been assumed to vary linearly in the lengthwise direction, while the radial field follows cubic variation for the displacements u and quartic variation for the displacement w.

For the attenuation error of less than 0.1% and for negligible phase shift the expansion parameter $p = 12$ permits the time step h to be as large as $0.498 T_m$ ($\omega^2 h^2 = 9.8$), where T_m is the period corresponding to the highest characteristic frequency of the 200 degree-of-freedom model shown in Fig. 5. This frequency is 3.8987×10^5 s^{-1}, so that the maximum time step h is limited to 0.8030×10^{-6} s. For convenience, however, a time step length of $h = 0.5\mu$s was used in the analysis. From the attenuation and phase shift analysis presented previously (see Figs. 4 and 5), it is evident that the integration procedure will introduce negligible errors into the results.

Some of the numerical results of this analysis are presented in Figs. 6, 7, and 8 and compared with previously published finite difference results obtained by Bertholf.[17] Comparison of radial displacements and longitudinal strains at the surface of the bar at stations located at $z = 2.54$ cm (1 in.), 5.08 cm (2 in.), and 7.62 cm (3 in.) from the free end indicates a good agreement between the two methods. The results of the transient response analysis demonstrate that the finite element

Table 2 Physical properties of the bar material

Length	254.0 mm (10 in.)
Diameter	25.4 mm (1 in.)
Young's modulus	72.395 GPa (10.5×10^6 lb/in.^{2})
Shear modulus	27.579 GPa (4.0×10^6 lb/in.^{2})
Density	2.7113×10^3 kg/m^3 (0.098 lb/in.^{3})
Poisson's ratio	0.3125

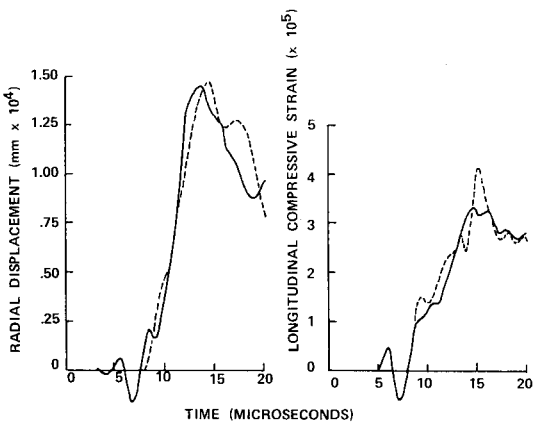

Fig. 7 Radial displacement and longitudinal strain at surface of bar at $z = 50.80$ mm (2 in.). ——, finite elements ($p = 12$); ----, finite difference (Ref. 17).

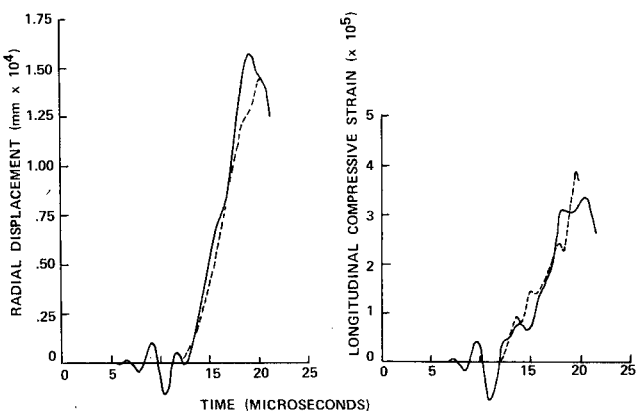

Fig. 8 Radial displacement and longitudinal strain at surface of bar at $z = 76.20$ mm (3 in.). ——, finite elements ($p = 12$); ----, finite difference (Ref. 17).

model response operator $D_p(h)$ with $p = 12$ can be used to assess the response characteristic of high-order idealizations of structural systems.

Concluding Remarks

The method described in this paper has been used to determine the short time response characteristics of a suddenly loaded elastic bar. The analysis was based on the approximation operator for $p = 12$. The results of this analysis clearly demonstrate that the present method can adequately represent a wave propagation response. The method has no inherent computational difficulties since only a single inversion of the mass matrix [see Eq. (9)] is required to obtain the approximation operator $D_p(h)$.

References

[1] Przemieniecki, J.S., *Theory of Matrix Structural Analysis,* McGraw-Hill, New York, 1968, p. 345.

[2] Fried, I., "Finite Element Analysis of Time-Dependent Phenomena," *AIAA Journal,* Vol. 7, June 1969, pp. 1170-1173.

[3] Argyris, J.H. and Scharpf, D.W., "Finite Elements in Time and Space," *The Aeronautical Journal,* The Royal Aeronautical Society, Vol. 73, Dec. 1969, pp. 1041-1044.

[4] Oden, J.T., "A General Theory of Finite Elements—II Applications," *International Journal of Numerical Methods in Engineering,* Vol. 1, 1969, pp. 247-259.

[5] Nickell, R.E., "On the Stability of Approximation Operators in Problems of Structural Dynamics," *International Journal of Solids and Structures,* Vol. 7, March 1971, pp. 301-319.

[6] Leech, J.W., Hsu, Pao-Tan, and Mack, E.W., "Stability of Finite Difference Method for Solving Matrix Equations," *AIAA Journal,* Vol. 3, Nov. 1965, pp. 2172-2173.

[7] Johnson, D.E., "A Proof of the Stability of the Houboult Method," *AIAA Journal,* Vol. 4, Aug. 1966, pp. 1450-1451.

[8] Geradin, M., "A Classification and Discussion of Integration Operators for Transient Structural Response," AIAA Paper 74-105, Feb. 1974.

[9] Trujillo, D.M., "The Direct Numerical Integration of Linear Matrix Differential Equations Using Padé Approximations," *International Journal for Numerical Methods in Engineering,* Vol. 9, 1975, pp. 259-270.

[10] Argyris, J.H., Dunne, P.G., and Angelopoulos, T., "Dynamic Response by Large Step Integration," *Earthquake Engineering and Structural Dynamics,* Vol. 2, 1973, pp. 185-203.

[11] Przemieniecki, J.S., *Theory of Matrix Structural Analysis,* McGraw-Hill, New York 1968, pp. 312-313.

[12] Frazer, P.A., Duncan, W.J., and Collar, A.R., *Elementary Matrices,* Cambridge University Press, New York, 1946, pp. 41-42, 209.

[13] Varga, R.S., *Matrix Iterative Analysis,* Prentice-Hall, Englewood Cliffs., N.J., 1962, p. 269.

[14] O'Brien, G.G., Hyman, M.A., and Kaplan, S., "A Study of the Numerical Solution of Partial Differential Equations," *Journal of Mathematics and Physics,* Vol. 29, 1951, pp. 223-251.

[15] Hohn, F.E., *Elementary Matrix Algebra,* Macmillan, New York, 1958, pp. 222-223.

[16] Przemieniecki, J.S., *Theory of Matrix Structural Analysis,* McGraw-Hill, New York, 1968, pp. 345-347.

[17] Bertholf, L.D., "Solution for Two-Dimensional Elastic Wave Propagation in Finite Bars," *Journal of Applied Mechanics,* Vol. 34, 1967, pp. 725-734.